

HIGH-TEMPERATURE HEAT EXCHANGE IN THE FLOW OF A
GAS IN A SLIT-TYPE QUENCHING APPARATUS

I. I. Borisov, V. V. Naumov,
T. V. Mikhalevskaya, and V. A. Reisig

UDC 533.6.011:536.24

A comparison is made of results of theoretical and experimental studies of high-temperature heat exchange in a slit-type quenching apparatus.

Due to the high rate at which the flow is cooled, a flow of relaxing gas in a quenching unit is accompanied by freezing of individual degrees of freedom of the particles. This leads to nonequilibrium distribution of the thermodynamic and thermophysical parameters of the medium in the channel of the unit and to a change in the normal heat-exchange conditions.

A good illustration of the above is experimental data on heat exchange and quenching of hot air in narrow slit-type channels [1].

As was justifiably noted in this work, it is a fairly difficult problem to calculate the parameters of a viscous, heat-conducting, relaxing high-gradient gas flow in a narrow slit when the thickness of the boundary layers is comparable to the thickness of the core. It is nearly impossible to measure velocity and temperature profiles in such a device.

The present work attempts to numerically obtain the distribution of the basic parameters inside a slit-type channel, including such complex parameters as the flow cooling rate. This data permits judgments to be made as to the character of the relaxation processes taking place, the freezing of the chemical composition [2], the vibration energy of the molecules [3], the temperature of free electrons [4], and the population of the levels for excited particles [5]. The integral characteristics obtained from the calculations were checked experimentally.

We studied the flow of hot argon in a plane slit channel with copper water-cooled walls of the following geometry: slit height at the channel inlet $1.5 \cdot 10^{-3}$ m, slit height at the channel outlet 10^{-3} m, slit width $20 \cdot 10^{-3}$ m, length $33 \cdot 10^{-3}$ m. The temperature of the argon at the inlet was varied within the range 1400–3000°K. The gas pressure was varied within the range $(1.34\text{--}1.36) \cdot 10^5$ Pa, and flow rate was held to a constant $2.75 \cdot 10^{-3}$ kg/sec. The gas was discharged into the atmosphere. The temperature of the channel wall was $\sim 300^\circ\text{K}$.

An approximate value of the gas cooling rate in the slit channel can be obtained from simultaneous solution of the equations for heat balance and convective heat transfer

$$\frac{dQ}{dx} = h s c_p u \frac{dT}{dx}, \quad \frac{dQ}{dx} = 2\alpha(h+s)(T-T_w). \quad (1)$$

If we consider that

$$\alpha = \frac{\lambda}{d_e} \text{Nu}, \quad d_e = 2 \frac{hs}{h+s}, \quad u \frac{dT}{dx} = \frac{dT}{dt}, \quad (2)$$

then from (1) it is easy to find the expression for the cooling rate

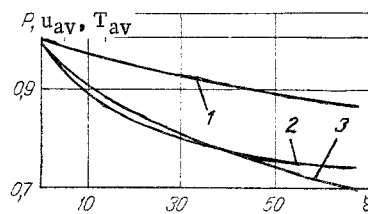


Fig. 1. Distribution of corrected transverse-mean integral parameters along the channel: 1) velocity; 2) temperature; 3) pressure.

Institute of Engineering Thermophysics, Academy of Sciences of the Ukrainian SSR, Kiev.
Translated from *Inzhenerno-Fizicheskii Zhurnal*, Vol. 43, No. 1, pp. 31-37, July, 1982.
Original article submitted March 30, 1981.

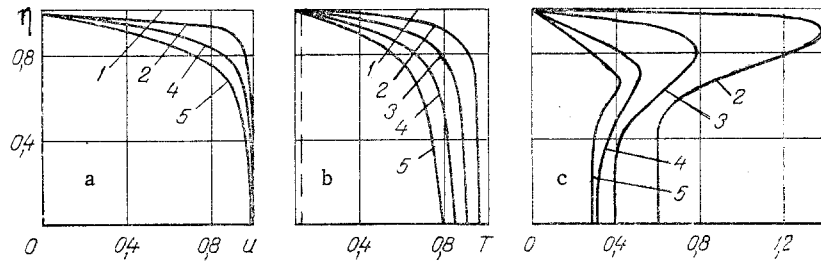


Fig. 2. Profiles of the longitudinal component of corrected velocity (a), temperature (b), and cooling rate (c) at different channel cross sections: 1) $\xi=0$; 2) 10; 3) 20; 4) 40; 5) 66. The quantity dT/dt is plotted off the x axis in Fig. 2c.

$$\frac{dT}{dt} = \frac{\lambda Nu}{\rho c_p} \left(\frac{h+s}{hs} \right)^2 (T - T_w). \quad (3)$$

Equation (3) was obtained without considering the work of expansion, which increases the cooling rate. It is apparent that in the case $s \gg h$ the cooling rate is inversely proportional to the square of the slit height and depends to a considerable degree on the temperature of the gas. For air with a temperature of $\sim 3000^\circ\text{K}$ at the inlet and a slit height of $1 \cdot 10^{-3}$ m, $dT/dt > 10^7$ deg/sec [1, 2].

With a decrease in slit height and an increase in gas temperature, viscous forces begin to prevent a further increase in cooling rate.

The traditional approach of using criterional relations requires the introduction of various empirical corrections and additional tests. We considered it more proper to use numerical methods to solve continuum equations of the Navier—Stokes type. This approach makes it possible to find both the longitudinal and transverse distributions of the parameters in a narrow slit-type channel.

We used the "slender channel" approximation [6, 7] as the mathematical model of the process. A distinctive feature of the flow in this case is that the thickness of the boundary layer is comparable to the height of the channel. Here there are low and moderate Reynolds numbers, when the effect of viscosity is manifest not only in the boundary layer, but over the entire flow field a relatively short distance after the inlet. If the channel can be accurately considered long ($h \ll l$, where h is the characteristic cross-sectional dimension and l is the length), then the flow of a viscous gas can be described using the system of "slender channel" equations, which coincide in form with the boundary-layer equations. The difference between these equations is as follows.

In the boundary-layer approximation, the distributions of pressure, velocity, and temperature are determined by solving the problem of inviscid external flow about a body, while the actual distribution is found by the iteration method with allowance for the displacement thickness. In the problem of the viscous flow of a gas in the approximation employing the "slender channel" model, the distribution is found as part of the general solution. Thus, the "slender channel" model is the next step in the direction of describing the field of the above-described flow within the framework of complete Navier—Stokes equations.

The basic system of equations (4) with boundary conditions (5) is written for an ideal gas and is supplemented by the condition of constant flow rate:

$$\begin{aligned} \rho u \frac{\partial u}{\partial \xi} + \rho w \frac{\partial u}{\partial \eta} &= - \frac{dP}{d\xi} + \frac{1}{\text{Re}} \frac{1}{y_w^2} \frac{\partial}{\partial \eta} \left(\mu \frac{\partial u}{\partial \eta} \right), \\ \frac{\partial}{\partial \xi} (y_w \rho u) + \frac{\partial}{\partial \eta} (y_w \rho w) &= 0, \quad \frac{dP}{d\eta} = 0, \\ \rho u \frac{\partial T}{\partial \xi} + \rho w \frac{\partial T}{\partial \eta} &= \frac{1}{\text{Re Pr}} \frac{1}{y_w^2} \frac{\partial}{\partial \eta} \left(\lambda \frac{\partial T}{\partial \eta} \right) + \text{Ec} \left(u \frac{\partial P}{\partial \xi} + \frac{1}{\text{Re}} \frac{1}{y_w^2} \mu \left(\frac{\partial u}{\partial \eta} \right)^2 \right), \\ \rho &= \frac{P \kappa M^2}{T}, \end{aligned} \quad (4)$$

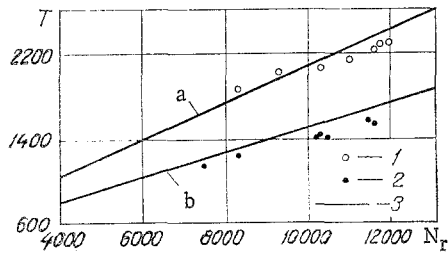


Fig. 3. Dependence of experimental values of temperature T (K) of argon flow on power N (W) of electric arc at the channel inlet (a) and outlet (b): 1) line reversal method; 2) thermocouple readings; 3) calorimetry.

$$u = 0, w = 0, T = T_w \text{ with } \eta = 1, \frac{\partial u}{\partial \eta} = 0, w = 0, \frac{\partial T}{\partial \eta} = 0 \text{ with } \eta = 0, \quad (5)$$

where $w = (v - y_w^1 \eta u) / y_w$, with the prime denoting differentiation with respect to x . All of the quantities in system (4) and boundary conditions (5) are dimensionless and relate to the below formulas. Here, for convenience in the numerical solution, we transformed the coordinate system so as to permit a changeover to a rectangular integration region:

$$\xi = \frac{x}{h}; \eta = \frac{y}{y_w(x)h}; u = \frac{u}{u_c}; v = \frac{v}{v_c}; P = \frac{P}{\rho_0 u_c^2};$$

$$\rho = \frac{\rho}{\rho_0}; T = \frac{T}{T_0}; \mu = \frac{\mu}{\mu_0}; \lambda = \frac{\lambda}{\lambda_0}.$$

As initial conditions, we chose single rectangular profiles for the temperature and longitudinal velocity component. It should be noted that there are two conditions for the vertical velocity component in this case, since the pressure is a function subject to determination.

System (4) with boundary conditions (5) was solved using the explicit scaling finite-difference method of Nikitenko [8].

In contrast to [8], the pressure distribution is found by the iteration method, with the introduction of relaxation coefficient β ($0.6 \leq \beta \leq 0.75$). This coefficient is linearly dependent on the gas temperature at the channel inlet and ensures convergence of the iteration process on physically acceptable results. The relations for the thermophysical parameters of the argon $\mu(T)$ and $\lambda(T)$ were approximated with second-degree polynomials.

Figure 1 shows the dimensionless distribution of pressure and transverse-mean integral velocity and temperature along the channel for gas parameters at the inlet $T_0 = 2500^\circ\text{K}$ and $P_0 = 1.365 \cdot 10^5$ Pa. Figure 2 shows profiles of the longitudinal velocity component, temperature, and cooling rate at different cross sections of the channel.

It is apparent that the dynamic and thermal boundary layers occupy about 40% of the cross section. The cooling rate distribution in the boundary layer has a distinct maximum and is several times greater at the inlet than in the core of the flow.

It can be concluded from analyzing the above relations that in the case of low catalytic activity of the channel wall material, the thermodynamic and thermophysical parameters of the relaxing medium in the boundary layer may be assumed frozen if the condition $c \cdot t^* \leq \tau_{rel}$ [9] is satisfied for the core of the flow.

The experiments were conducted on a plasma stand which included a 30-kW plasmatron, cylindrical damping chamber with a transitional convergent duct at the slit aperture, the slit-type quenching apparatus, and a slit-type diagnostic attachment made of refractory ceramic. The cathode of the plasmatron was made of tungsten and was pressed into a copper holder. The anode was copper, and eddy stabilization of the arc was employed. The input and output characteristics of the hot flow in the slit channel were determined by measuring all of the electrical and thermal parameters of the electric-arc heater (from panel instruments), the flow rate of the gas and cooling water (using RS-5 rotameters), and the gas pressure (using standard manometers). The water temperature was measured with mercury thermometers installed in organic glass holders. The gas temperature at the channel inlet was determined by calorimetry of the cathode and anode components of the plasmatron and the damping chamber.

To monitor the thermal balance for different plasmatron operating regimes, we measured the temperature of the flow by using the D-resonance line of sodium. The tests were conducted in the current range 100–300 A at a voltage of 50–60 V and a constant 2.75 g/sec rate of

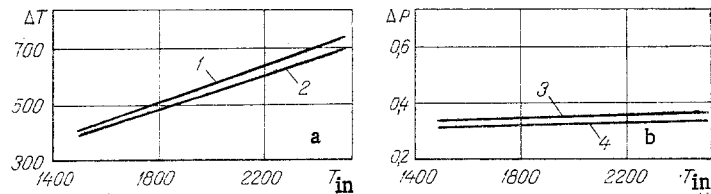


Fig. 4. Dependence of gradient of temperature (a) and pressure (b) in the quenching unit on the temperature at the inlet: 1, 3) test data; 2, 4) calculated values. $P, 10^5 \text{ Pa}$.

flow of the plasma-generating gas — argon. The walls of the damping chamber were washed with an NaCl solution. The line was adjusted with an SPM-2 monochromator with a quartz prism. An FEU-62 indicator was used. The signal was recorded on a GIB1 recorder. The standard source was an SI8-200 lamp. The moment of reversal of the line, corresponding to equality of the thermodynamic temperature of the flow core to the brightness temperature of the source, was determined graphically at the point of intersection of the curves of radiant intensity of the source and the total intensity of the gas + source.

The gas temperature beyond the slit channel was also determined by two methods: from the heat balance, and with a platinum-platinorhodium thermocouple installed in a ceramic attachment at the channel outlet so that the velocity of the forward flow would be at the level 100-150 m/sec [10].

It follows from Fig. 3 that the spread due to determination of the mass-mean temperature of the flow by different methods is no greater than 10%.

Comparison of the results of the calculation and the test data on the gas temperature and pressure drop in the channel of the quenching unit is offered in Fig. 4.

The good agreement between the data (difference no more than 7%) shows that the chosen approach of numerically modeling the process of flow and heat transfer in a slit channel is correct. The quenching-unit characteristics obtained in the present work indicate the promise of the use of narrow slit-type channels for rapid nonadiabatic cooling of high-temperature gas flows.

NOTATION

x, y , distances measured along axis and along normal to axis; ξ, η , longitudinal and transverse coordinates in the rectangular integration region; h, s, l , height, width, and length of slit channel; d_e , equivalent diameter of the channel; $y_w(x)$, contour equation; $\rho, c_p, \kappa, \lambda, \mu$, density, heat capacity, adiabatic exponent, thermal conductivity, and absolute viscosity of gas, respectively; T, P , temperature and pressure of gas; T_w , temperature of wall; u, v , longitudinal and transverse velocity components; Q , quantity of heat; α , heat-transfer coefficient; Re, Pr, Nu, Ec, M , Reynolds, Prandtl, Nusselt, Eckert, and Mach numbers, respectively; t, τ_{rel}, t_* , time, relaxation time of physicochemical process, characteristic time scale; c , constant of the order of unity. Indices: w , value of parameters on the wall; av , mean value; 0 , value of quantity on the channel axis in the initial section.

LITERATURE CITED

1. É. A. Sakalauskiene, G. Yu. Linkaitite, and P. Yu. Valatkyavichus, "Heat transfer in the turbulent flow of diatomic high-temperature gases in narrow channels," in: Problems of High-Temperature Heat and Mass Transfer, ITMO Akad. Nauk Bel. SSR, Minsk (1979), pp. 84-92.
2. V. A. Reisig, S. A. Stadnik, and G. M. Shchegolev, "High-temperature fixation of nitrogen oxides," *Khim. Vys. Energ.*, 1, No. 6, 587-590 (1967).
3. B. F. Gordiets, A. I. Osipov, and L. A. Shelepin, *Kinetic Processes in Gases and Molecular Lasers* [in Russian], Nauka, Moscow (1980).
4. S. Bairon, P. Borts, and G. Rassel, "Theory of nonequilibrium plasmas," in: Applied Magnetohydrodynamics [Russian translation], Mir, Moscow (1965), pp. 273-294.
5. L. I. Gudzenko and S. I. Yakovlenko, *Plasma Lasers* [in Russian], Atomizdat, Moscow (1978).

6. I. C. Williams, "Viscous compressible and incompressible flow in slender channels," AIAA J., 1, No. 1, 215-224 (1963).
7. Ray, "Certain results of numerical calculations of viscous flows of a rarified gas in nozzles in a slender-channel approximation," Raket. Tekh. Kosm., 9, No. 5, 52-62 (1971).
8. N. I. Nikitenko, Investigation of Heat-Transfer Processes by the Grid Method [in Russian], Naukova Dumka, Kiev (1978).
9. S. A. Losev, Gas Lasers [in Russian], Nauka, Moscow (1977).
10. M. I. Pevzner and A. S. Isserlin, "Pyrometer for accurate measurements of the temperature of dust-free flows," in: Radiant Heat Exchange (Methods and Instruments for Studying Radiant Heat Exchange) [in Russian], Kaliningrad University, Kaliningrad (1974), pp. 183-189.

CHEMICAL REACTIONS, HEAT EXCHANGE AND FAST PARTICLES

A. A. Abramov and N. K. Makashev

UDC 533.6.011

We give results of a numerical and analytical study of the effect of the "tails" of the distribution function, i.e., the solution of the model Bkhatnagar—Gross—Krook equation, on the rate of a high-threshold reaction and on the heat flux.

It is known that many chemical reactions have a high energy barrier and take place in collisions of molecules whose velocities of motion are much larger than the average thermal velocity. The validity of the Chapman—Enskog solution of the Boltzmann equation which is the basis for the Euler equation, Navier—Stokes equation, etc., is limited by the conditions $k = l_0/L \ll 1$, $mc^2 \sim 2kT$ (see, e.g., [1, 2]). Taking into account large energies of translational motion of the particles requires that one gives up the familiar concepts about the properties of kinetic equations for $k \ll 1$. In particular, the molecular distribution function f of molecules which interact with potential $U_{ij} = B_{ij}r^{1-s}$, $s > 2$, differs considerably from the Maxwell distribution f_0 , and is nonlocal for $c \gg c^* = cTk^{-\beta/2}$, $\beta = (s - 1)/(s + 1)$. It is important to note for a further investigation that in the last estimate, the Knudsen number is determined from the scale of change of the gas parameters (e.g., its temperature) by a magnitude.

Thus, one can expect that in spatially inhomogeneous flows, the rate constant of a high-threshold reaction will differ considerably from the equilibrium value [2]. In addition, the increase of k reduces the region in the space of molecular velocities where the difference between f and f_0 is small, and where the Chapman—Enskog solution is valid. This in turn is reflected in the increase of the direct effect of the "tail" properties of the distribution functions on the gas dynamics.

The direct effect here means the effect of the deviation of f from the Chapman—Enskog solution on the reaction rate, heat flux, stress tensor, etc., which are calculated from f . We note that the effect can also be indirect. For example, because of the change in the description of the kinetics of high-threshold reactions, the solution will give different concentration fields of the components and, as a result, different values of the transfer coefficients. This phenomenon will not be considered here. In this work we use the example of heat exchange between two infinite parallel plates at temperature T_{1W} and $T_{2W} > T_{1W}$ in the

TABLE 1. Comparison of the Analytical and Numerical Solutions

V_∞		2,5	5,0	7,5	10	12,5
$x_1 = 0,265$	$\Phi_{1,num}^{(+)}$	0,882	0,364	0,142	0,0655	0,0347
$k = 0,0245$	$\Phi_{1,an}^{(+)}$	0,888	0,369	0,143	0,0659	0,0348

Translated from Inzhenerno—Fizicheskii Zhurnal, Vol. 43, No. 1, pp. 37-43, July, 1982. Original article submitted April 3, 1981.